Freshwater in the Bay of Bengal

Its Fate and Role in Air-Sea Heat Exchange

By Amala Mahadevan, Gualtiero Spiro Jaeger,
Mara Freilich, Melissa M. Omand,
Emily L. Shroyer, and Debasis Sengupta

Photo credit: Gualtiero Spiro Jaeger

ABSTRACT. The strong salinity stratification in the upper 50–80 m of the Bay of Bengal affects the response of the upper ocean to surface heat fluxes. Using observations from November to December 2013, we examine the effect of surface cooling on the temperature structure of the ocean in a one-dimensional framework. The presence of freshwater adds gravitational stability to the density stratification and prevents convective overturning, even when the surface becomes cooler than the subsurface. This stable salinity stratification traps heat within subsurface layers. The ocean's reluctance to release the heat trapped within these subsurface warm layers can contribute to delayed rise in surface temperature and heat loss from the ocean as winter progresses. Understanding the dispersal of freshwater throughout the bay can help scientists assess its potential for generating the anomalous temperature response. We use the Aquarius along-track surface salinity and satellite-derived surface velocities to trace the evolution and modification of salinity in the Lagrangian frame of water parcels as they move through the bay with the mesoscale circulation. This advective tracking of surface salinities provides a Lagrangian interpolation of the monthly salinity fields in 2013 and shows the evolution of the freshwater distribution. The along-trajectory rate of salinification of water as it leaves the northern bay is estimated and interpreted to result from mixing processes that are likely related to the host of submesoscale signatures observed during our field campaigns.

INTRODUCTION

The Bay of Bengal and its surrounding coastal region receive the highest rainfall in the world (Figure 1). As a consequence of the heavy rainfall and terrestrial run-off from several large rivers, including the Ganges, Brahmaputra, and Irrawaddy, the Bay of Bengal is one of the freshest subtropical ocean regions in the world. The majority of the freshwater input occurs along the bay's northeastern margins and results in a strong lateral salinity gradient at the surface. The increase in surface salinity due to evaporation is far short of the freshening by precipitation and runoff; thus, in order for the bay to maintain its salinity over the years, there must be a net export of freshwater through boundary currents, mesoscale circulation, and eddy fluxes, aided by diapycnal mixing, to balance the input of freshwater.

The fresher water that enters the Bay of Bengal resides mostly in a near-surface layer. In contrast to most other low- and mid-latitude oceans, salinity, rather than temperature, strongly controls the density gradient in the upper 50–80 m. Only at depths greater than 80–100 m is temperature consistently the dominant control on density gradients. Temperature inversions can occur and persist within a region where salinity dictates density stratification (Gopalakrishna et al., 2005; Thadathil et al., 2007). In many parts of the northern Bay of Bengal where the effects of freshwater dominate, we find layers of warm water trapped beneath cooler surface water. This is particularly striking during the winter months, November to February, when north-easterly winds cool the ocean's surface and freshwater covers the northern bay. During this period, the observed salinity is in the range of 26–31 psu on average. Just as heat can remain trapped subsurface in winter due to salinity dictating the density stratification, it can also build up in the subsurface on a diel time scale. Daytime shortwave heating decays exponentially with depth, but nighttime cooling occurs at the surface. If near-surface salinity stratification inhibits convective overturning when the surface is being cooled, heat can build up subsurface even while it is lost near the surface. Thus, both on seasonal and diel time scales, density stratification resulting from freshwater input can alter the upper ocean's response to air-sea heat flux. Sea surface temperature (SST) evolves differently in the presence of dominating salinity stratification, and since SST and air-sea heat fluxes feed back on one another, the freshwater in the Bay of Bengal has a profound effect on both SST and air-sea heat fluxes (Parampil et al., 2010; Thangaprakash et al., 2016, in this issue).

What role does the low salinity of surface waters in the Bay of Bengal play in the ocean's response to heat fluxes? In the first part of this article, we address this question through analysis of observations from the Bay of Bengal. Using example profiles of salinity and temperature from a recently collected data set, we demonstrate how salinity stratification affects the evolution of the upper-ocean temperature profile in response to a specified heat flux. We also examine the effect of a prescribed air temperature on heat loss from the ocean. These simple one-dimensional analyses are thought experiments based on our observations. Further studies that examine the three-dimensional effects of heat exchange with the atmosphere, as well as the coupled feedback on air-sea fluxes, are underway and will be reported in forthcoming articles. In the second part of this article, we aim to better understand the annual distribution of freshwater within the bay and the mechanisms by which the freshwater is dispersed. The evolution of salinity in the Bay of Bengal on an annual time scale has been addressed by several modeling (Benshila et al., 2014; Akhil et al., 2014; Wilson and Riser, 2016) and observational (Sengupta et al., 2006; D'Addezio et al., 2015; Pant et al., 2015) studies, while considering the transport of freshwater. Here, we combine sea surface salinity from the Aquarius satellite mission with altimeter-derived sea surface velocity to interpret the time evolution of the surface salinity distribution. By calculating Lagrangian trajectories of water parcels in the surface ocean and interpolating Aquarius along-track salinity data onto these Lagrangian trajectories (Jönsson et al., 2009), we map the

dynamically evolving surface salinity field over the year 2013. Further, by tracking the rate of change of salinity along the Lagrangian trajectories of water parcels, we identify where the salinity is being modified along the advective pathway, possibly through submesoscale or small-scale processes that are not reflected in the mesoscale dynamics.

Our understanding of the freshwater distribution in the Bay of Bengal, and the mechanisms for its dispersal, have been greatly enhanced through the Air-Sea Interactions Regional Initiative (ASIRI) US Office of Naval Research Departmental Regional Initiative (Lucas et al., 2014; Wijesekera et al., in press) in collaboration with India's Ocean Mixing and Monsoon (OMM) program. Here, we use data from a ship survey conducted from R/V *Roger Revelle* during the period November 28–December 13, 2013. This cruise, one of several cruises conducted as part of the ASIRI-OMM collaboration, mapped temperature and salinity in the upper 200 m of the ocean at unprecedented resolution (roughly

2 km spacing in the horizontal and 1 m deep bins in the vertical) over a large extent of the international waters in the bay (Figure 2a). The cruise track covered approximately 3,500 km and consisted of four legs that formed a bow-tie shape extending roughly between 7°N–18°N and 84°E–90°E, with the longest leg oriented more or less south to north. Eighty-six conductivity-temperature-depth (CTD) profiles were recorded at 81 stations, which included water sampling to a depth of 220 m at a nominal spacing of 20 nm (37 km) along the ship's track. Temperature and salinity were nearly continuously profiled to a depth of 220 m using an Oceanscience UnderwayCTD (uCTD) while transiting at a speed of 10–12 knots. About 10 vertical profiles of temperature and salinity were recorded every hour, giving a nominal horizontal spacing of 1 nm (~1.9 km) between profiles. Satellite-derived products, such as sea level anomaly, surface winds, surface velocity, sea surface temperature (SST), and sea surface salinity (SSS) from the Aquarius mission,

contributed a great deal in guiding the in situ observations and in understanding the large-scale variability in this region.

EFFECTS OF FRESHWATER ON AIR-SEA HEAT EXCHANGE
Response of Temperature to Surface Cooling

To illustrate the effects of salinity stratification on the evolution of the upper-ocean temperature structure in the Bay of Bengal, we compare two temperature-salinity (T-S) profiles, one from the northern bay that is more strongly influenced by freshwater and the other from the southern bay (Figure 2), collected using the uCTD system on board R/V *Roger Revelle* from November 28–December 13, 2013. The data were processed into 1 m vertical bins, which form the vertical grid cells for these simple numerical experiments in which the vertical profiles of T and S are evolved, as described. Each set of profiles is subject to a weak and steady heat flux (cooling) of $Q = -50$ W m^{-2} for a period of 21 days. The temperature in the surface grid cell is modified appropriately
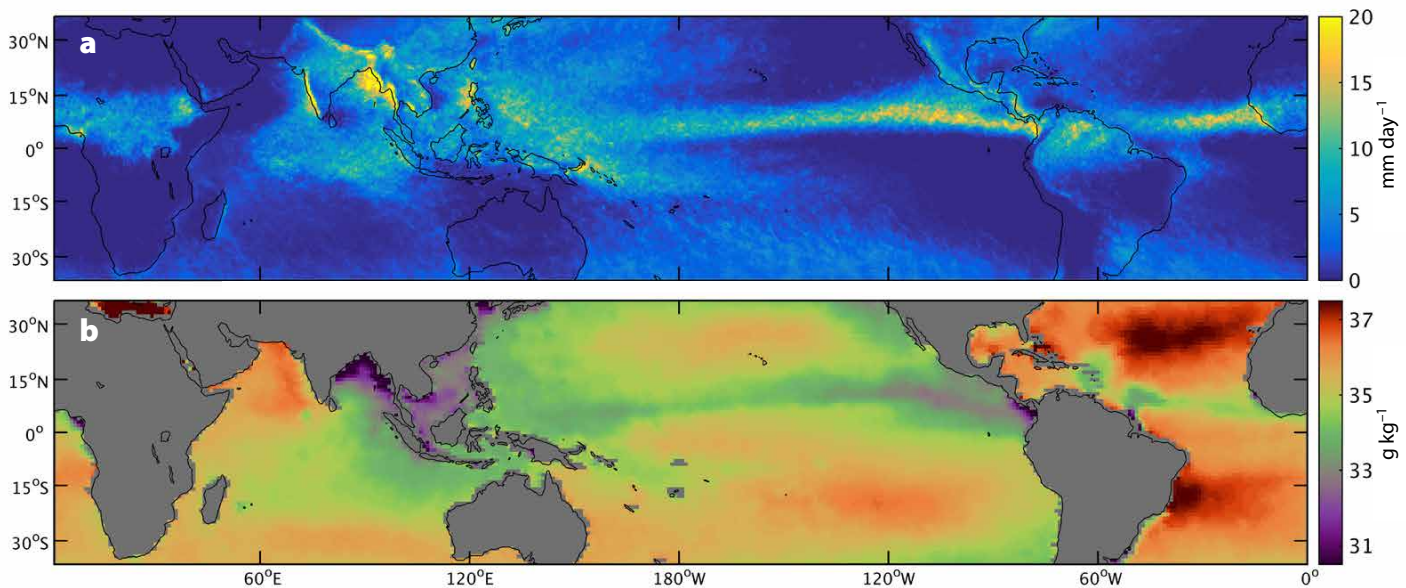

FIGURE 1. (a) Climatological rainfall for the month of July (mm day^{-1}) derived from the Tropical Rainfall Measuring Mission (TRMM) satellite, and (b) sea surface salinity (SSS) from the Aquarius satellite for October. July is the peak of the southwest summer monsoon and the time of maximum precipitation, whereas October is the time when the lowest surface salinities are observed in the Bay of Bengal, as the river runoff that follows the heavy summer monsoon makes its impression in the ocean salinity. The peak rainfall and freshwater input strongly influence the annual mean climatology of rainfall and SSS, and show similar patterns, with lower annually averaged values. The Aquarius salinity data were obtained from the NASA EOSDIS Physical Oceanography Distributed Active Archive Center (PO.DAAC) at the Jet Propulsion Laboratory, Pasadena, CA (NASA Aquarius Project, 2015; Lee et al., 2012). The TRMM rainfall data were obtained from the NASA GES DISC at the Goddard Space Flight Center (http://daac.gsfc.nasa.gov; Wang et al., 2014).

to account for the heat loss from the surface bin during each time increment of the numerical integration. A small vertical diffusivity of 10^{-5} m^2 s^{-1} is applied in conjunction with the T and S profiles. Density is calculated from the nonlinear equation of state, and if the density profile is gravitationally unstable, convective adjustment is applied repeatedly, starting from the surface and working downward, until static equilibrium is achieved. This is repeated in time increments of 260 seconds for a period of 21 days. The evolution of two different T and S vertical profiles (Figure 2b,c) referred to as P1 and P2, taken from the south and north bay, respectively, show a marked difference. Profile P1 near 11°N shows the presence of a shallow, 7 m deep, fresh layer with a salinity of 32.7 psu (Figure 2b). The salinity difference, $\Delta S = 0.5$ psu as compared to the salinity just below this layer, creates a density difference $\Delta\rho = -\beta\Delta S$ that makes this layer statically stable. When the surface is cooled, the temperature drops rapidly by more than a degree; yet, the convection does not penetrate the

strong halocline at 7 m because the density change is not sufficient to overcome $\Delta\rho$. With further cooling, the temperature is lowered sufficiently by an amount ΔT, such that its effect on density $\alpha\Delta T$ overcomes the stable density stratification provided by salinity, $-\beta\Delta S$. For a constant cooling rate q W m^{-2}, the temperature change (ΔT) achieved over a mixed layer depth (H) in time Δt is $\Delta T = q\Delta t/(\rho C_p H)$, where ρ and C_p are the density and specific heat capacity of the seawater, respectively, and q is negative. Thus, the time taken to achieve the drop in temperature ΔT that overcomes the halocline's density differential is

$$\Delta t = -\frac{\rho C_p H}{q}\frac{\beta\Delta S}{\alpha},$$

which in this case is about 10 days. Only then does convective overturning mix the temperature and salinity of the surface layer with those of the subsurface layer, relatively abruptly, to a depth of 40 m in this case, where the overturning is arrested by another halocline (Figure 2b). Vertical mixing brings up the

warmer subsurface water, and the surface temperature rises in spite of the heat loss applied to the surface, as can be seen in the time evolution of SST (red line in Figure 2d). In contrast, profile P2 near 17°N (Figure 2c) exhibits a more or less uniform rate of surface cooling as heat is removed from the surface (Figure 2c,d). Here too, the presence of a halocline prevents the cooler near-surface water from mixing with the warmer subsurface water at 20 m. Further cooling or strong wind-induced mixing would be required to extract the heat trapped between 20 m depth and 75 m depth.

Extraction of Heat from Subsurface Warm Layers

During the November–December 2013 cruise, we frequently found temperature inversions where coherent warm layers existed below cooler surface waters (Figure 3). The 1,250 km long, south-to-north transect (Leg A on the map in Figure 2a) showed that the surface waters were much fresher in the northern bay (Figure 3a), where the largest
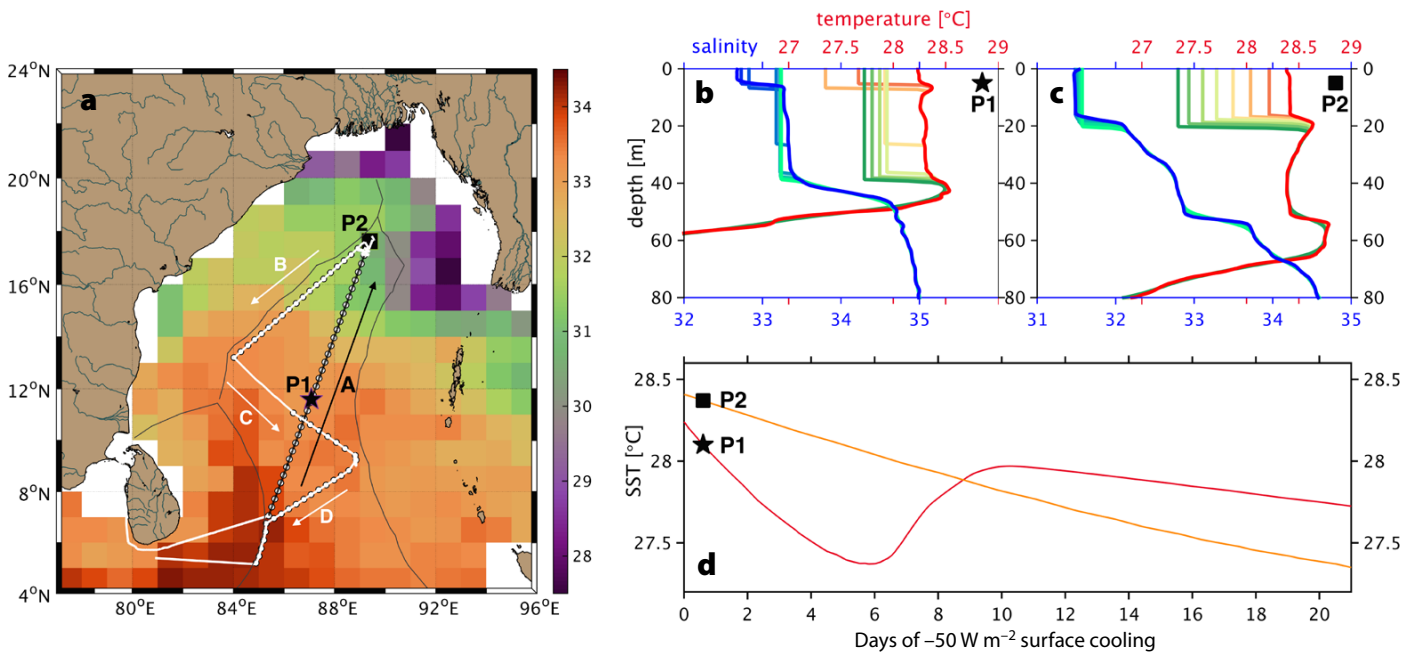

FIGURE 2. (a) Map of the Bay of Bengal showing average sea surface salinity for November–December from the Aquarius satellite gridded data (color) and the November 28–December 13, 2013, cruise track of R/V *Roger Revelle* (white line, with section A highlighted in black). Salinity and temperature profiles representative of two different scenarios (P1 indicated by the black star and P2 by the square) are picked from Section A of the cruise (emphasized in black). The initial profiles of salinity (blue) and temperature (red) from profiles (b) P1 and (c) P2 are used to evolve a simple model in which the surface is cooled. The temperature and salinity profiles are evolved in time increments that ensure static stability at each time (described in the text). The two cases—(b) for profile P1 and (c) for profile P2—evolve differently, as shown by the progression in the colored lines set apart by three days in (b) and (c). (d) Time-evolution of sea surface temperature for P1 (red), and P2 (orange).

subsurface thermal maxima occurred (Figure 3b). During this time period, the net heat flux turned negative (the ocean was cooling) in the northern bay, and the combined latent and longwave cooling at night exceeded the shortwave heating during the day. However, the surface cooling did not penetrate deeply, especially in the northern bay. The amount of heat contained above the 28°C isotherm (black line in Figure 3a,b) is greater in the northern bay as compared to the southern bay, even though the SST is slightly lower in the north. This heat, stored above the 28°C isotherm, is calculated as

$$Q_{28} = \rho\, Cp \int_{z(28°C)}^{0} (T(°C) - 28°C)\, dz$$

and is plotted in Figure 3c. The choice of 28°C is meant merely to be illustrative, and another temperature value within the range of upper-ocean temperatures could also be considered in the same way. In order to examine how readily the ocean might release its heat to the atmosphere, we perform a simple experiment on each of the vertical profiles that make up the
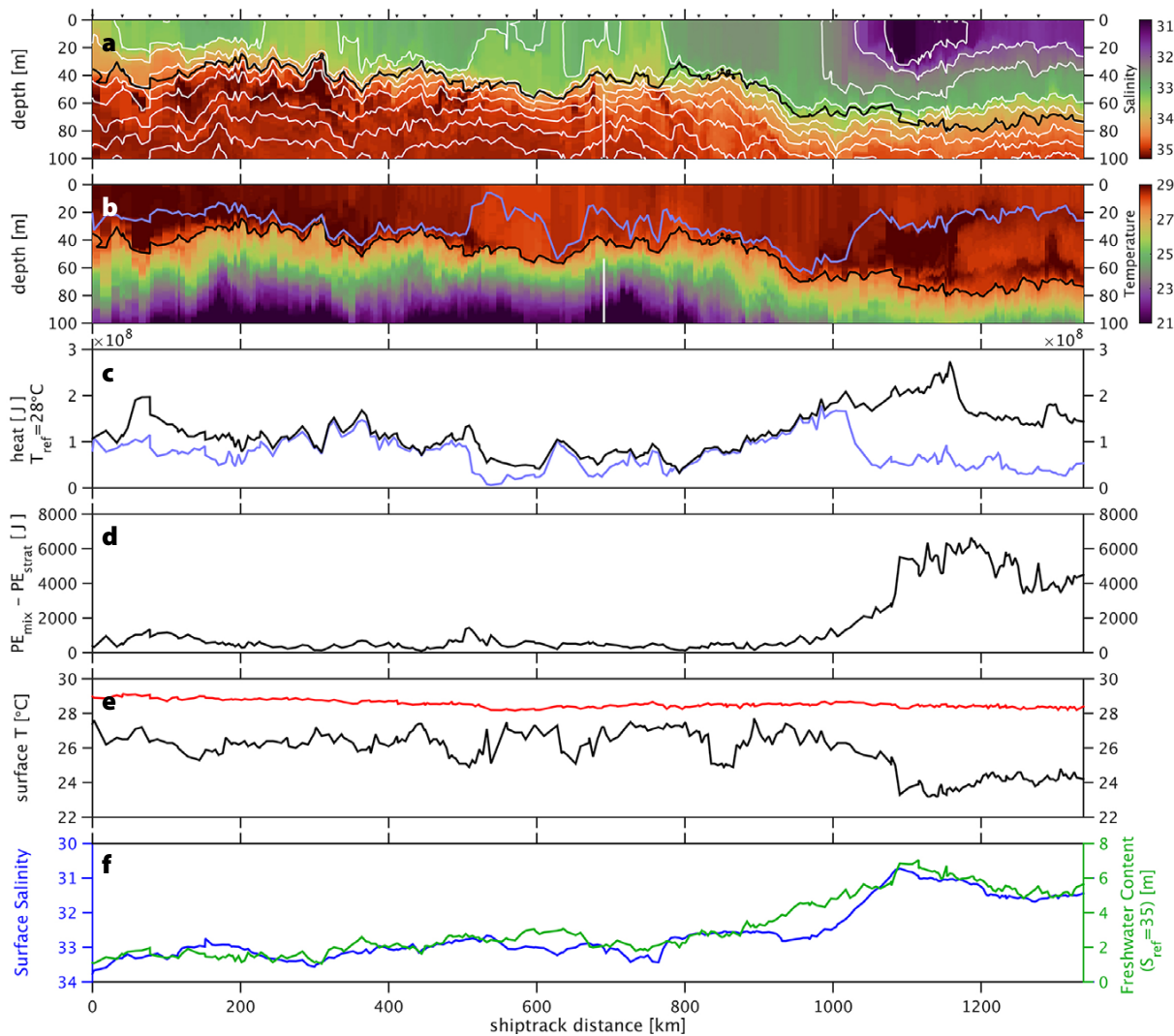

FIGURE 3. Section A of the cruise (track shown in Figure 2a) showing (a) salinity and (b) temperature measured with an underway CTD system on board R/V *Revelle* from November 28 to December 13, 2013. The data consist of profiles to a depth of 200 m (only the upper 100 m are shown) at a spacing of approximately 3 km along track. The data are binned to 1 m in the vertical. Fresher water originating from river runoff is evident at the surface in the northern part of the section (right-hand side). Temperature inversions, with subsurface layers being warmer than the surface, are seen in the salinity-stratified region to the north, and intrusions of saline water are seen subsurface in the southern part of the section. (c) The black line shows the amount of heat contained above the 28°C isotherm (indicated by the black contour in (b)). The blue line shows the amount of heat extracted when the sea surface temperature (SST) is held at 28°C. The depth to which convective mixing would occur is indicated by the blue line in (b). (d) The difference between the potential energy of the density profiles and the state where the ocean is vertically mixed from the surface to the depth of the 28°C isotherm (see text). (e) The black line is the SST with which the surface needs to be forced in order for convective mixing to reach the depth of the 28°C isotherm. The red line is the actual unaltered SST. (f) The green line is the freshwater content (H_{FW} in m) and the blue line is sea surface salinity (SSS in psu). The two are strongly correlated, with a cross-correlation coefficient of 0.95.

T-S section in Figure 3a,b. We assume the surface air temperature is 28°C and allow the ocean to equilibrate by losing heat (to the atmosphere) at the surface and using convective adjustment to regain static stability whenever the vertical profile of density becomes convectively unstable. The blue line in Figure 3b is the depth to which convective mixing penetrates when SST is held at 28°C, and it is substantially shallower than the 28°C isotherm in places of strong salinity stratification. The blue line in Figure 3c indicates the amount of heat extracted from the ocean as a result. A large fraction of the total heat above the 28°C isotherm (the difference between the black and the blue lines in Figure 3c) remains trapped subsurface and is, in fact, the reason that we see more heat content in the northern bay at this time. The salinity stratification limits the depth of convection and maintains a stable density profile even with temperature inversions. Figure 3d shows a measure of the stratification present in the mixed or inverted temperature layer. It is the difference in potential energy (*PE*) between the initial (stratified) and adjusted (mixed) profile, where

$$PE = \int_{z(28°C)}^{0} (\rho - \rho_0)gdz$$

is integrated above the local depth of the 28°C isotherm. Homogenizing the density above the isotherm generates the mixed state. How much would the surface need to cool for convective mixing to penetrate through this salinity stratification? We repeat the previous experiment by forcing (lowering) the surface temperature of the profiles, allowing them to convectively adjust, and incrementally decreasing the forced surface temperature of each profile until convective adjustment reaches the 28°C isotherm. The black line in Figure 3e shows the forced surface temperature required to attain this state, while for comparison, the red line shows the original observed surface temperatures of the profiles. The difference indicates that although the surface temperature of the northern bay is

observed to be nearly 28°C, it would need to cool by more than 4°C for convective mixing to break through the salinity stratification and extract heat to the depth of the 28°C isotherm. Alternatively, mechanical mixing driven by a strong wind event, such as a cyclone, can potentially tap into subsurface waters that are several degrees warmer than the surface.

These analyses show the substantial influence of freshwater on the ocean's response to a cooling atmosphere. The anomalous temperature response and subsurface trapping of heat is related to the freshwater content. The freshwater content, H_{FW}, expressed in meters of freshwater, is calculated with respect to a reference salinity S_{ref} as

$$H_{FW} = \int_{z(S_{ref})}^{0} \frac{(S(z) - S_{ref})}{S_{ref}dz}.$$

Here, $z(S_{ref})$ is the depth of the isohaline S_{ref}, which could be chosen as any isohaline that lies well bellow the freshwater-influenced layer. Figure 3f shows H_{FW} for the observed salinity profiles, where $S_{ref} = 35$ psu. It is the height of a column of pure freshwater that would be generated by extracting all of the freshwater at depths above the S_{ref} isohaline, leaving a residual salinity of 35 psu. The strong correlation between the freshwater content H_{FW} and surface salinity (cross-correlation coefficient = 0.95) suggests that the modification of freshwater occurs through lateral mixing, or a combination of surface spreading and vertical mixing processes, as described below. In the following, we discuss the modification of freshwater as it makes its way out of the bay.

Modification of Salinity

The lateral salinity gradient results in strong density fronts that are dynamically active (MacKinnon et al., 2016, in this issue), form eddies, and slump. In the process, they transform horizontal density gradients into vertical density gradients and enhance the density stratification. One can imagine several processes by which the salinity of the

fresher water increases as it spreads from north to south (Figure 4) across the bay. Each of these processes modifies SSS and H_{FW} in different ways. (a) If the layer of fresher water at the surface is mixed vertically (diapycnally) with the subsurface layers (Figure 4a), SSS would increase, but H_{FW} of the water column would remain unchanged. (b) If a region of freshwater that is separated from saltier water (both vertically and horizontally) by a mixed layer front is mixed horizontally (Figure 4b), the SSS in the fresher region would increase, but the column-integrated H_{FW} would decrease on the fresher side. (c) If, on the other hand, the freshwater front were to slump and spread laterally at the surface without mixing, H_{FW} would decrease on the fresher side,

(a) Vertical mixing

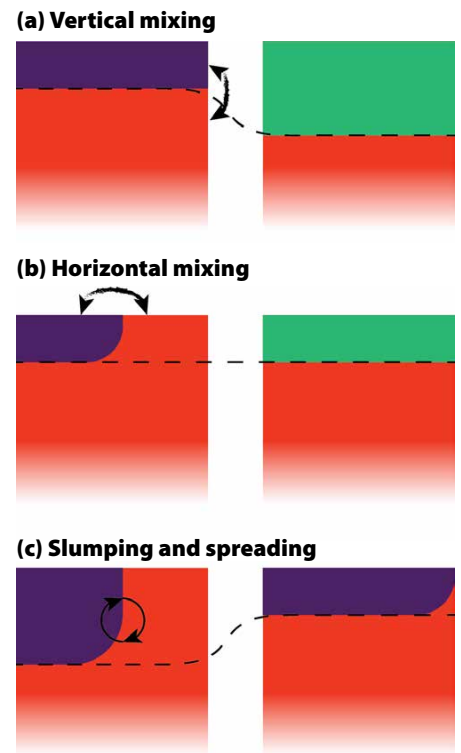**(b) Horizontal mixing**

(c) Slumping and spreading

FIGURE 4. This schematic illustrates the way in which vertical and horizontal processes can change the sea surface salinity. (a) Vertical mixing increases sea surface salinity (SSS) but not the depth-integrated freshwater content (H_{FW}). (b) Horizontal mixing across a front increases SSS and decreases the depth-integrated freshwater content at a point that was formerly in the freshwater region. (c) Slumping and spreading of a front does not change SSS, but decreases H_{FW} on what was originally the fresher side of the front.

but SSS would remain unchanged.

Of these processes, we believe that lateral mixing, or some combination of slumping and vertical mixing, modifies the freshwater as it makes its way across the bay. This is suggested by the fact that SSS and H_{FW} are strongly correlated throughout the bay (Figure 3). Vertical mixing remains suppressed by the freshwater stratification except during hurricanes, and to some extent during the southwest monsoon (Shroyer et al., 2016, in this issue). A Lagrangian analysis of satellite SSS described in the following sections also suggests salinity modification along the advective pathways that freshwater takes in leaving the bay. Our observations support the widespread prevalence of submesoscale processes in the bay (MacKinnon et al., and Lucas et al., 2016, both in this issue), which could potentially contribute to mixing between fresher and saltier water. But, the precise mechanisms that facilitate freshwater mixing and modification are not yet well understood (Sarkar et al., 2016, in this issue).

DISTRIBUTION OF FRESHWATER

We use SSS from the Aquarius satellite to map the distribution of freshwater and to examine the evolution of the salinity field over the annual cycle in 2013. A dynamic interpolation method (Jönsson et al., 2009) is used to reconstruct the surface salinity. It advects Aquarius satellite along-track SSS using satellite altimeter-derived sea surface velocity. This method reveals a dynamically evolving spatial and temporal variability in SSS that is not captured through the typical binning or compositing of data for creating gridded monthly products. Though Aquarius salinity measurements are limited in their spatial resolution, we find satellite along-track lateral salinity gradients to be representative of ship-based measurements at spatial scales greater than 9 km, the mean distance between Aquarius measurements along track. However, the lack of reliable salinity and velocity fields near the coast makes it difficult to capture the largest salinity gradients. Each panel in Figure 5 shows particles labeled with SSS measurements from the first to the twentieth day of each month, moved in the mesoscale flow field to their projected positions on the twentieth day of each month. Objective mapping is used to fill gaps. This reconstructed SSS shows evidence of eddy transport, with filaments of fresher water drawn out from the coastal regions throughout the year. SSS in the northern Bay of Bengal is less than 33 psu
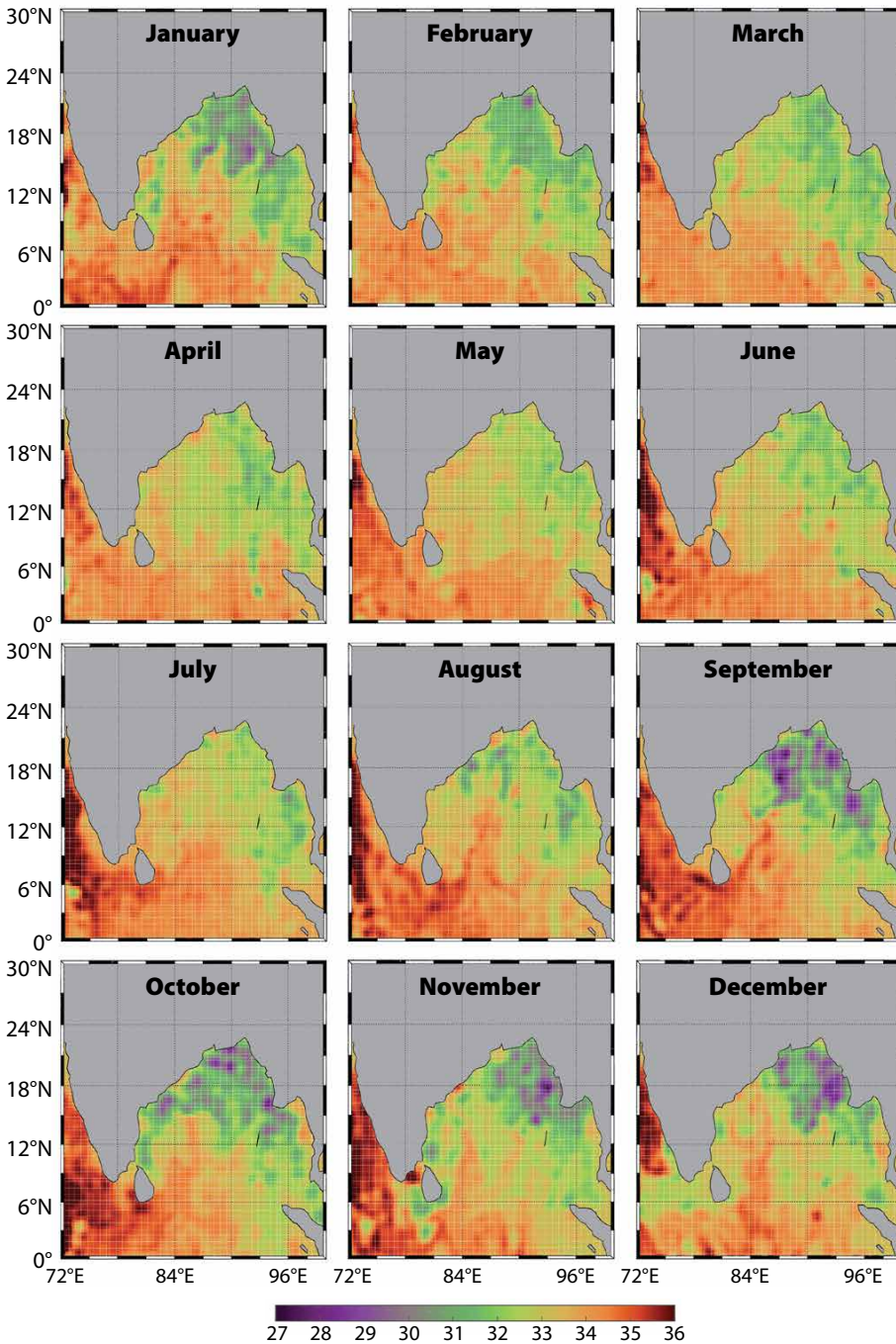

FIGURE 5. Salinity for the twentieth day of each month in 2013 reconstructed from Aquarius satellite data and surface geostrophic velocities from Ocean Surface Current Analyses Real-time (OSCAR; Bonjean and Lagerloef, 2002). The images are generated by objective mapping of the field generated by Lagrangian interpolation. It uses an algorithm that relaxes to the mean when no data are available within the decorrelation length scale, so the salinity values along the coast, where no Aquarius data are available, are unrealistic.

throughout the year. During and after the summer monsoon (June to August), high-salinity waters from the Arabian Sea can be seen entering the bay (Jensen, 2001; Vinayachandran et al., 2013; Wijesekera et al., 2016, in this issue) with the Summer Monsoon Current (SMC). The SMC flows northeastward from the western Arabian Sea, south of Sri Lanka, and into the eastern Bay of Bengal from May to September, and is dominated by Ekman drift and remote wind forcing from the equatorial Indian Ocean (Shetye et al., 1996; Schott and McCreary, 2001; Shankar et al., 2002). The high-salinity signal in the southwest bay is less noticeable after October, when the SMC reverses direction to flow westward.

An offshore salinity minimum appears near the mouths of the Ganges-Brahmaputra and Irrawaddy Rivers in August and is strongest in September. In most years, the low salinity appearing at the 18°N mooring (Weller et al., 2016, in this issue) originates from the Ganges-Brahmaputra outflow in September. The salinity minimum near the mouth of the Irrawaddy in the eastern bay is carried northwest for the most part and appears at the 18°N mooring site in December (Gordon et al., 2016, in this issue), although a low-salinity signal propagates south into the Andaman Sea as well. Low-salinity water first appears south of 12°N in the eastern bay in August. Southward advection of low-salinity waters by the East India Coastal Current (EICC) along the western boundary of the bay (Shetye et al., 1993) is seen from September to November. Patches of low-salinity water remain visible at the bay's boundaries from December to February. High-salinity water enters the bay from the Arabian Sea from July to October. Surface freshwater in the northeastern bay becomes saltier earlier than that in the northwestern bay. The northeastern bay SSS is around 31–32 psu from March to June, right before the onset of the summer monsoon, while the northwestern bay SSS is around 32–33 psu in the same months.

FATE OF FRESHWATER

To examine the rate of freshwater modification, we must account for its circulation by the mesoscale flow field, which is known to be important in this region (Rao and Sivakumar, 2003). Rates of change of salinity are estimated along water parcel trajectories calculated with the Ocean Surface Current Analyses Realtime (OSCAR; Bonjean and Lagerloef, 2002; Dohan and Maximenko, 2010) altimeter- and wind-derived flow field, which has been evaluated against data in the Indian Ocean (Sikhakolli et al., 2013). Along-track Aquarius SSS is cast in the Lagrangian frame by attaching the salinity data to virtual particles advected by the flow (Jönsson et al., 2009, 2011). When the advecting particles intercept a newly laid down SSS track, their values are updated using linear interpolation in time along the particle trajectory. The rate of change of salinity (material derivative) is thereby calculated along the path taken by the water as it is advected through the bay. We estimate the material derivative using two consecutive measurements of salinity, S_1 and S_2 at times t_1 and t_2, respectively, along the trajectory of a water parcel, as

$$\frac{DS}{Dt} = \frac{S_2 - S_1}{t_2 - t_1}. \tag{1}$$

This Lagrangian rate of change of salinity (DS/Dt) can be ascribed to several processes described by

$$\frac{DS}{Dt} = \frac{\partial S}{\partial t} + \nabla \cdot (uS) = \kappa \nabla^2 S + w_e(S - S_b) + \frac{E - P}{h} S + V_o, \tag{2}$$

where u is the horizontal velocity of the water, E is evaporation, P is precipitation, h is the mixed layer depth, and w_e is the entrainment velocity at the mixed layer depth. S_b is the salinity just below the mixed layer, and V_o is the rate of change of surface salinity due to vertical processes other than entrainment. When discussing sea surface salinity, the vertical term also includes subduction and upwelling, although these processes do not change

the properties of a water mass in the three-dimensional Lagrangian frame.

To assess the net effect of these processes in modulating the surface salinity as water transits through the bay (Akhil et al., 2014), we composite all the values of DS/Dt calculated over three-month periods of 2013 into 1/3 × 1/3 degree grid cells. The rate of change in salinity along water parcel trajectories evolves seasonally and displays some coherent spatial variability. The annual maximum Lagrangian rate of change in salinity is a salinification of 0.4 psu per day that occurs along the western margin of the bay from August to October, as southwestward-flowing riverine water mixes with saltier water (Figure 6a). There are relatively fast currents, shallow mixed layer depths, and a thick barrier layer in the region during this time (Thadathil et al., 2007). There is also upwelling close to the coast due to Ekman drift, and all these factors could lead to an increase in salinity through lateral or vertical mixing. However, the coarse-resolution mesoscale flow field used here for estimating advection does not resolve submesoscale processes and could underestimate the residence time of water, or conversely, its velocity. During the late-summer to postmonsoon period, a distinct band of freshening is apparent in the southwestern bay, a region of strong currents that appears to overlap with the SMC (Figure 6a). As water enters the Bay of Bengal from the Arabian Sea, it becomes fresher at a rate of 0.1 psu per day. An alternative interpretation is that the saltier water entering the bay subducts below a fresh surface layer, but the satellite surface data are not sufficient to identify this pathway.

From July to November, water entering the northeastern bay freshens for the most part due to surface fluxes and river runoff (Han et al., 2001). The highest precipitation is over the northeastern bay from June to September. While precipitation is reduced post-monsoon, there is net precipitation over a shallow mixed layer in the northeastern bay through October (Figure 6b). However,

$$\frac{DS}{Dt} = \frac{\partial S}{\partial t} + \nabla \cdot (uS) = \kappa \nabla^2 S + w_e(S - S_b) + \frac{E - P}{h} S + V_o$$
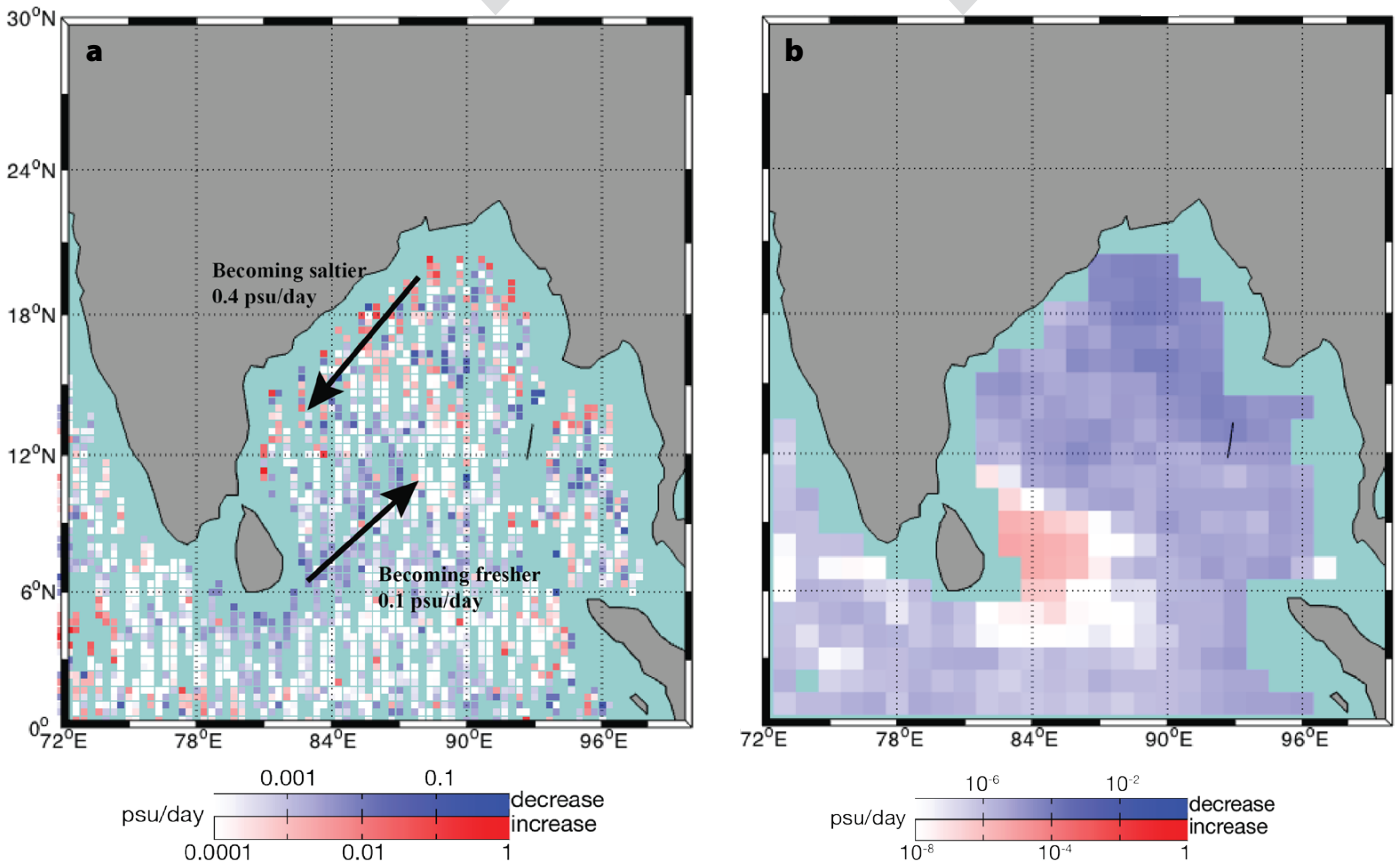

FIGURE 6. (a) Lagrangian rate of change in salinity composited onto a 1/3 × 1/3 degree grid for the period August to October 2013. Arrows indicate general direction of currents. (b) Rate of change of mixed layer salinity due to surface fluxes constructed from observations of precipitation (NASA TRMM data), evaporation (Yu and Weller, 2007), and mixed layer depth (Schmidtko et al., 2013). Note the logarithmic color bars. The contribution of the surface fluxes is negligible in comparison to the advective change.

the average precipitation-driven increase in salinity is an order of magnitude less than the estimated change in salinity along trajectories. Because precipitation occurs on short time scales, intense freshening is possible, but not captured, in the seasonal mean. Throughout the year, there is only weak southward transport from the northeastern bay. The mean circulation in the northeastern bay during and after the summer monsoon results in northwestward transport of water from the Irrawaddy River.

SUMMARY

The large input of freshwater that the Bay of Bengal receives along its northern margins has no way to leave other than to be transported south. The freshwater stratification, strongest in the north and enhanced in the fall and early winter, suppresses convective overturning. Stratification alters the temperature response of the upper ocean to heat fluxes. A significant amount of heat (that may have been acquired during the summer months) can remain trapped subsurface for substantial periods of time (months) even during winter. The longer-term fate of this subsurface heat and its potential for latent heating and evaporation at later times in the year is being further examined.

Reconstruction of the spatial and temporal (monthly) variability of sea surface salinity from satellite data shows freshwater dispersal by the mesoscale flow field. Because vertical diapycnal mixing is highly suppressed by the strong density stratification induced by freshwater, the salinification of the fresher water as it is transported out of the bay is likely influenced by lateral mixing processes associated with submesoscale instabilities. By tracking SSS from the along-track Aquarius data in the Lagrangian frame of surface velocity, we identify the regions where the salinity is modified most rapidly along its advective pathway. 🌀

REFERENCES
Akhil, V.P., F. Durand, M. Lengaigne, J. Vialard, M.G. Keerthi, V.V. Gopalakrishna, C. Deltel, F. Papa, and C. de Boyer Montégut. 2014. A modeling study of the processes of surface salinity seasonal cycle in the Bay of Bengal. *Journal of Geophysical Research Oceans* 119:3,926–3,947, http://dx.doi.org/10.1002/2013JC009632.

Benshila, R., F. Durand, S. Masson, R. Bourdallé-Badie, C. de Boyer Montégut, F. Papa, and G. Madec. 2014. The upper Bay of Bengal salinity structure in a high-resolution model. *Ocean Modelling* 74:36–52, http://dx.doi.org/10.1016/j.ocemod.2013.12.001.

Bonjean, F., and G.S. Lagerloef. 2002. Diagnostic model and analysis of the surface currents in the tropical Pacific Ocean. *Journal of Physical Oceanography* 32(10):2,938–2,954, http://dx.doi.org/10.1175/1520-0485(2002)032<2938:DMAAOT>2.0.CO;2.

D'Addezio, J.M., B. Subrahmanyam, E.S. Nyadjro, and V.S.N. Murty. 2015. Seasonal variability of salinity and salt transport in the northern Indian Ocean. *Journal of Physical Oceanography* 45(7):1,947, http://dx.doi.org/10.1175/JPO-D-14-0210.1.

Dohan, K., and N. Maximenko. 2010. Monitoring ocean currents with satellite sensors. *Oceanography* 23(4):94–103, http://dx.doi.org/10.5670/oceanog.2010.08.

Gopalakrishna, V.V., Z. Johnson, G. Salgaonkar, K. Nisha, C.K. Rajan, and R.R. Rao. 2005. Observed variability of sea surface salinity and thermal inversions in the Lakshadweep Sea during contrasting monsoons. *Geophysical Research Letters* 32, L18605, http://dx.doi.org/10.1029/2005GL023280.

Gordon, A.L., E.L. Shroyer, A. Mahadevan, D. Sengupta, and M. Freilich. 2016. Bay of Bengal: 2013 northeast monsoon upper-ocean circulation. *Oceanography* 29(2):82–91, http://dx.doi.org/10.5670/oceanog.2016.41.

Han, W., J.P. McCreary, and K.E. Kohler. 2001. Influence of precipitation minus evaporation and Bay of Bengal rivers on dynamics, thermodynamics, and mixed layer physics in the upper Indian Ocean. *Journal of Geophysical Research* 106(C4):6,895–6,916, http://dx.doi.org/10.1029/2000JC000403.

Jensen, T. 2001. Arabian sea and Bay of Bengal exchange of salt and tracers in an ocean model. *Geophysical Research Letters* 28:3,967–3,970, http://dx.doi.org/10.1029/2001GL013422.

Jönsson, B., J. Salisbury, and A. Mahadevan. 2009. Extending the use and interpretation of ocean satellite data using Lagrangian modeling. International *Journal of Remote Sensing* 30(13):3,331–3,341, http://dx.doi.org/10.1080/01431160802558758.

Jönsson, B., J. Salisbury, and A. Mahadevan. 2011. Large variability in continental shelf production of phytoplankton carbon revealed by satellite. *Biogeosciences* 8:1,213–1,223, http://dx.doi.org/10.5194/bg-8-1213-2011.

Lee, T., G. Lagerloef, M. Gierach, H.-Y. Kao, S. Yueh, and K. Dohan. 2012. Aquarius reveals salinity structure of tropical instability waves. *Geophysical Research Letters* 39, L12610, http://dx.doi.org/10.1029/2012GL052232.

Lucas, A.J., J.D. Nash, R. Pinkel, J.A. MacKinnon, A. Tandon, A. Mahadevan, M.M. Omand, M. Freilich, D. Sengupta, M. Ravichandran, and A. Le Boyer. 2016. Adrift upon a salinity-stratified sea: A view of upper-ocean processes in the Bay of Bengal during the southwest monsoon. *Oceanography* 29(2):134–145, http://dx.doi.org/10.5670/oceanog.2016.46.

Lucas, A., E. Shroyer, H.W. Wijesekera, H.J.S. Fernando, E. D'Asaro, M. Ravichandran, S. Jinadasa, J.A. MacKinnon, J.D. Nash, R. Sharma, and others. 2014. Mixing to monsoons: Air-sea interactions in the Bay of Bengal. *Eos, Transactions American Geophysical Union*, 95(30):269–270, http://dx.doi.org/10.1002/2014EO300001.

MacKinnon, J.A., J.D. Nash, M.H. Alford, A.J. Lucas, J.B. Mickett, E.L. Shroyer, A.F. Waterhouse, A. Tandon, D. Sengupta, A. Mahadevan, and others. 2016. A tale of two spicy seas. *Oceanography* 29(2):50–61, http://dx.doi.org/10.5670/oceanog.2016.38.

NASA Aquarius Project. 2015. Aquarius Official Release Level 3 Sea Surface Salinity Standard Mapped Image Monthly Climatology Data V4.0. PO.DAAC, CA, http://dx.doi.org/10.5067/AQR40-3SUCS.

Pant, V., M.S. Girishkumar, T.V.S.U. Bhaskar, M. Ravichandran, F. Papa, and V.P. Thangaprakash. 2015. Observed interannual variability of near-surface salinity in the Bay of Bengal. *Journal of Geophysical Research* 120:3,315–3,329, http://dx.doi.org/10.1002/2014JC010340.

Parampil, S.R., A. Gera, M. Ravichandran, and D. Sengupta. 2010. Intraseasonal response of mixed layer temperature and salinity in the Bay of Bengal to heat and freshwater flux. *Journal of Geophysical Research* 115, C05002, http://dx.doi.org/10.1029/2009JC005790.

Rao, R.R., and R. Sivakumar. 2003. Seasonal variability of sea surface salinity and salt budget of the mixed layer of the north Indian Ocean. *Journal of Geophysical Research* 108(C1), 3009, http://dx.doi.org/10.1029/2001JC000907.

Sarkar, S., H.T. Pham, S. Ramachandran, J.D. Nash, A. Tandon, J. Buckley, A.A. Lotliker, and M.M. Omand. 2016. The interplay between submesoscale instabilities and turbulence in the surface layer of the Bay of Bengal. *Oceanography* 29(2):146–157, http://dx.doi.org/10.5670/oceanog.2016.47.

Schmidtko, S., G.C. Johnson, and J.M. Lyman. 2013. MIMOC: A global monthly isopycnal upper-ocean climatology with mixed layers. *Journal of Geophysical Research* 118(4)1,658–1,672, http://dx.doi.org/10.1002/jgrc.20122.

Schott, F.A., and J.P. McCreary Jr. 2001. The monsoon circulation of the Indian Ocean. *Progress in Oceanography* 51(1):1–123, http://dx.doi.org/10.1016/S0079-6611(01)00083-0.

Sengupta, D., G.N. Bharath Raj, and S.S.C. Shenoi. 2006. Surface freshwater from Bay of Bengal runoff and Indonesian throughflow in the tropical Indian ocean. *Geophysical Research Letters* 33, L22609, http://dx.doi.org/10.1029/2006GL027573.

Shankar, D., P. Vinayachandran, and A. Unnikrishnan. 2002. The monsoon currents in the north Indian Ocean. *Progress in Oceanography* 52(1):63–120, http://dx.doi.org/10.1016/S0079-6611(02)00024-1.

Shetye, S., A. Gouveia, D. Shankar, S. Shenoi, P. Vinayachandran, D. Sundar, G. Michael, and G. Nampoothiri. 1996. Hydrography and circulation in the western Bay of Bengal during the northeast monsoon. *Journal of Geophysical Research* 101(C6):14,011–14,025, http://dx.doi.org/10.1029/95JC03307.

Shetye, S., A. Gouveia, S. Shenoi, D. Sundar, G. Michael, and G. Nampoothiri. 1993. The western boundary current of the seasonal subtropical gyre in the Bay of Bengal. *Journal of Geophysical Research* 98(C1):945–954, http://dx.doi.org/10.1029/92JC02070.

Shroyer, E.L., D.L. Rudnick, J.T. Farrar, B. Lim, S.K. Venayagamoorthy, L.C. St. Laurent, A. Garanaik, and J.N. Moum. 2016. Modification of upper-ocean temperature structure by subsurface mixing in the presence of strong salinity stratification. *Oceanography* 29(2):62–71, http://dx.doi.org/10.5670/oceanog.2016.39.

Sikhakolli, R., R. Sharma, S. Basu, B. Gohil, A. Sarkar, and K. Prasad. 2013. Evaluation of OSCAR ocean surface current product in the tropical Indian Ocean using in situ data. *Journal of Earth System Science* 122(1):187–199, http://dx.doi.org/10.1007/s12040-012-0258-7.

Thadathil, P., P.M. Muraleedharan, R.R. Rao, Y.K. Somayajulu, G.V. Reddy, and C. Revichandran. 2007. Observed seasonal variability of barrier layer in the Bay of Bengal. *Journal of Geophysical Research Oceans* 112, C02009, http://dx.doi.org/10.1029/2006JC003651.

Thangaprakash, V.P., M.S. Girishkumar, K. Suprit, N. Suresh Kumar, D. Chaudhuri, K. Dinesh, A. Kumar, S. Shivaprasad, M. Ravichandran, J.T. Farrar, and others. 2016. What controls seasonal evolution of sea surface temperature in the Bay of Bengal? Mixed layer heat budget analysis using moored buoy observations along 90°E. *Oceanography* 29(2):202–213, http://dx.doi.org/10.5670/oceanog.2016.52.

Vinayachandran, P., D. Shankar, S. Vernekar, K. Sandeep, P. Amol, C. Neema, and A. Chatterjee. 2013. A summer monsoon pump to keep the Bay of Bengal salty. *Geophysical Research Letters* 40(9):1,777–1,782, http://dx.doi.org/10.1002/grl.50274.

Wang, J.-J., R.F. Adler, G.J. Huffman, and D. Bolvin. 2014. An updated TRMM composite climatology of tropical rainfall and its validation. *Journal of Climate* 27:273–284, http://dx.doi.org/10.1175/JCLI-D-13-00331.1.

Weller, R.A., J.T. Farrar, J. Buckley, S. Mathew, R. Venkatesan, J. Sree Lekha, D. Chaudhuri, N. Suresh Kumar, and B. Praveen Kumar. 2016. Air-sea interaction in the Bay of Bengal. *Oceanography* 29(2):28–37, http://dx.doi.org/10.5670/oceanog.2016.36.

Wijesekera, H.W., E. Shroyer, A. Tandon, M. Ravichandran, D. Sengupta, S.U.P. Jinadasa, H.J.S. Fernando, N. Agarwal, K. Arulanathan, G.S. Bhat, and others. In press. ASIRI: An ocean-atmosphere initiative for Bay of Bengal. *Bulletin of the American Meteorological Society*, http://dx.doi.org/10.1175/BAMS-D-14-00197.1.

Wijesekera, H.W., W.J. Teague, E. Jarosz, D.W. Wang, T.G. Jensen, S.U.P. Jinadasa, H.J.S. Fernando, L.R. Centurioni, Z.R. Hallock, E.L. Shroyer, and J.N. Moum. 2016. Observations of currents over the deep southern Bay of Bengal—with a little luck. *Oceanography* 29(2):112–123, http://dx.doi.org/10.5670/oceanog.2016.44.

Wilson, E.A., and S.C. Riser. 2016. An assessment of the seasonal salinity budget for the upper Bay of Bengal. *Journal of Physical Oceanography* 46(5):1,361–1,376, http://dx.doi.org/10.1175/JPO-D-15-0147.1.

Yu, L., and R.A. Weller. 2007. Objectively analyzed air-sea heat fluxes for the global ice-free oceans (1981–2005). *Bulletin of the American Meteorological Society* 88:527–539, http://dx.doi.org/10.1175/BAMS-88-4-527.

AUTHORS
Amala Mahadevan (amala@whoi.edu) is Senior Scientist, Woods Hole Oceanographic Institution, Woods Hole, MA, USA. **Gualtiero Spiro Jaeger** and **Mara Freilich** are graduate students in the MIT/WHOI Joint Program in Oceanography, Cambridge/Woods Hole, MA, USA. **Melissa M. Omand** is Assistant Professor, Graduate School of Oceanography, University of Rhode Island, Narragansett, RI, USA. **Emily L. Shroyer** is Assistant Professor, College of Earth, Ocean, and Atmospheric Sciences, Oregon State University, Corvallis, OR, USA. **Debasis Sengupta** is Professor, Centre for Atmospheric and Oceanic Sciences, Indian Institute of Science, Bangalore, India.